J Mater Sci (2008) 43:6020–6023
DOI 10.1007/s10853-008-2883-8

LETTER

Production of an austenitic steel matrix composite reinforced by in-situ nodular eutectic: the role of Si

Zhenming Xu · Gaofei Liang

Received: 9 October 2007 / Accepted: 16 July 2008 / Published online: 11 August 2008

Particle-reinforced metal matrix composites have higher strength and wear resistance than that of its matrix material because the particle phases impart resistance to abrasive wear [1–4]. However, these materials are generally not widely used due to the complex manufacturing processes required coupled with high costs. Austenitic steel has been widely used as a wear-resistant material because austenite exhibits excellent strain hardening under high energy impact wear [5]. Yet, it has poor wear resistance under low-to-medium energy impact wear. White cast iron has high wear resistance because the eutectic carbide can strongly resist abrasive wear but it suffers from low strength and poor toughness. To overcome these deficiencies, a new type of austenitic steel matrix wear-resistant composite reinforced by in situ nodular eutectics, was created [6]. These composites possess the advantages of an austenite matrix coupled with the wear resistant of white cast iron. This composite shows high strength, high toughness, and high wear resistance [6]. Till this time, thermodynamics of forming the eutectic and the effect of Si on the solidification behavior of this composite has not been studied in detail. The aim of this research was to develop a new method for producing this steel matrix composite reinforced with an in situ nodular eutectic by controlling the solidification structure of the steel. Furthermore, the effect of Si on thermodynamics of formation of the eutectic in this composite has been examined. This provides a new method for controlling the solidification products from the steel melt.

The chemical compositions of the steels were (wt.%): 1.20–1.50C, 6.00–10.00Mn, 0.032P, and 0.025S. The steel was prepared via a non-oxidation process with a 5 kg induction furnace. When the temperature reached 1600 °C, Al was added to the melt, and the steel was poured. The Si–Fe compound (2 wt.%Ce, 75 wt.%Si, and 23 wt.%Fe) was added to the ladle prior to pouring. Samples of dimensions $\Phi 8 \times 100$ mm^2 were cast in metallic molds. Specimens for microstructural evaluation were prepared using conventional metallographic techniques and subsequently etched in 5% Nital. An electron probe microanalyzer (DX4) was used to characterize the composites. The unidirectional solidified bar was ground to $\Phi 7 \times 100$ mm^2 in size. The unidirectional solidification experiment was performed using a high temperature gradient Bridgman-type unit in protective argon atmosphere. The solidification rate was 450 μm/s. A detailed description of the unit is provided elsewhere [7].

Figure 1 shows the microstructures of Fe–1.50 wt.%C–8.00 wt.%Mn composite with added 1.13 wt.%Si, 1.50 wt.%Si, 1.88 wt.%Si, and 2.05 wt.%Si, respectively. Nodular eutectics are dispersed in the austenite matrix in the as-cast state, as shown in Fig. 1. The volume fraction of the eutectic in the as-cast structure increased as the Si content increased as follows: 4.50 wt.%®6.50 wt.%®8.60 wt.%® 11.80 wt.%. The proportion of nodular-shaped eutectics increased with the increment of Si and was dispersed in the austenite matrix in the as-cast state. Figure 2 shows the microstructure of longitudinal section for the unidirectional solidified Fe–1.25 C–6.60 Mn–1.06 Si composite at solidification rate of 450 μm/s. Numerous nodular-shaped eutectics are dispersed between austenitic grains (A arrow) and austenitic dendrite arms (B and C arrows).

The nodular eutectic of the composite is the $(Fe,Mn)_3C$ and austenite (γ-Fe) eutectic [8]. Electron probe microanalysis revealed that the chemical composition of the eutectic is (wt.%) 1.83–2.35C, 6.94–11.75Mn, and 1.97–2.23Si. When

Z. Xu (✉) · G. Liang
School of Environmental Science and Engineering, Shanghai Jiao Tong University, 800 Dongchuan Road, Shanghai 200240, People's Republic of China
e-mail: zmxu@sjtu.edu.cn

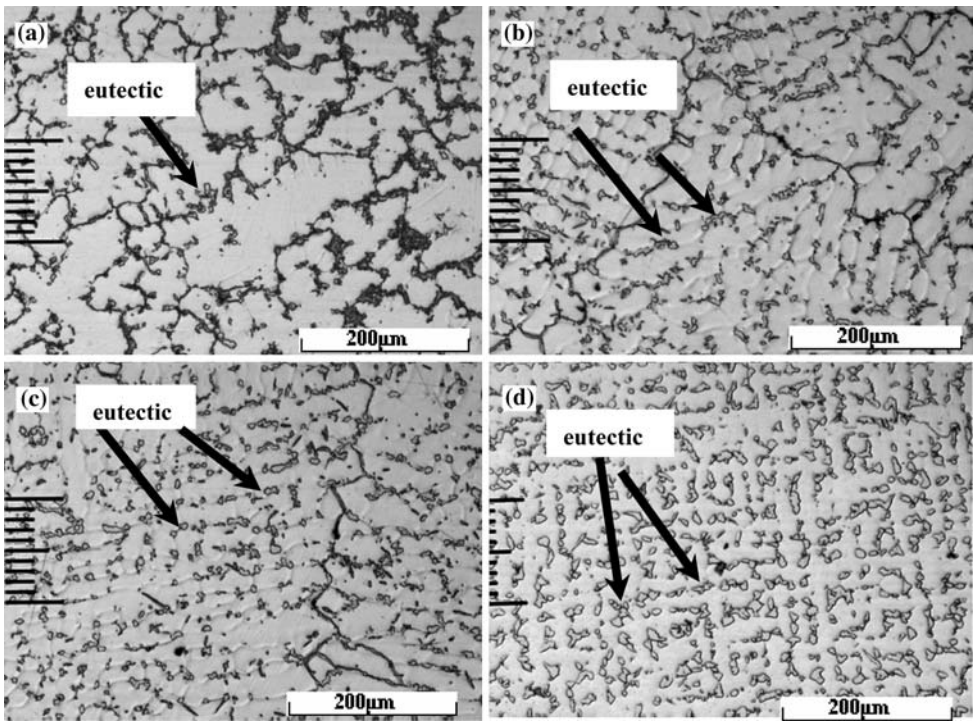

Fig. 1 Microstructure of Fe–1.50 wt.%C–8.00 wt.% Mn composite with the different Si contents. (**a**) 1.13 wt.%Si, (**b**) 1.50 wt.%Si, (**c**) 1.88 wt.%Si, (**d**) 2.05 wt.%Si

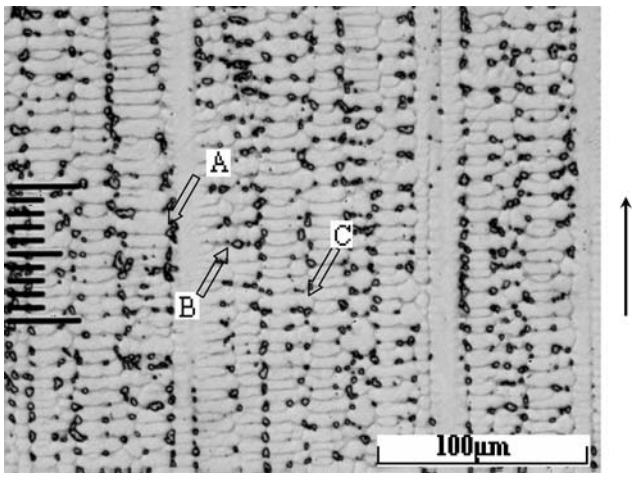

Fig. 2 Microstructure of longitudinal section of the unidirectionally solidified Fe–1.25C–6.60 Mn–1.06 Si composite produced at solidification rate of 450 μm/s (Arrow indicating growth direction)

the eutectic solidifies, the $(Fe,Mn)_3C$ is formed [9]. The ΔG (Gibbs energy) for formation of $(Fe,Mn)_3C$ is:

$$3[Fe] + 3[Mn] + [C] = (Fe,Mn)_3C \tag{1}$$

$$\Delta G = \Delta G^0 + RT \ln \frac{1}{a^3_{Fe,L}(T) a^3_{Mn,L}(T) a_{C,L}(T)} \tag{2}$$

where ΔG^0 is standard Gibbs energy, $a_{Fe,L}(T)$ is the activity for solute Fe in the fluid phase at temperature T, $a_{Mn,L}(T)$ is the activity for solute Mn in the fluid phase at temperature T, $a_{C,L}(T)$ is the activity for solute C in the fluid phase at temperature T.

Fe is solvent, it is taken at $f_{Fe,L}(T) = 1$(the activity coefficients for solute Fe in the fluid phase) [10] in the calculation.

Equation 2 changes to

$$\Delta G = \Delta G^0 - RT[3 \ln w(Fe)_L + 3 \ln w(Mn)_L + \ln w(C)_L + 6.908 \lg f_{Mn,L}(T) + 2.303 \lg f_{C,L}(T)] \tag{3}$$

and

$$\lg f_{Mn,L}(T) = e^{Mn}_{Mn} w(Mn)_L + e^{C}_{Mn} w(C)_L + e^{Si}_{Mn} w(Si)_L$$

where $f_{i,L}(T)$is the activity coefficients for solute i in the fluid phase. $f_{i,L}(T)$ is calculated using Eq. 4.

The activity coefficient of C in Fe–C–Mn–Si alloy austenite (solid phase) is [11]:

$$\lg f_{C,S}(T) = \frac{2300}{T} - 2.24 + \frac{180 + 8.90 w(Si)_S}{T} w(C)_S + (0.041 + \frac{62.5}{T}) w(Si)_S - \frac{21.8}{T} w(Mn)_S \tag{4}$$

where e^C_C, e^{Mn}_C, and e^{Si}_C are the interaction coefficients of activity of C, Mn, and Si, respectively. The values of e^C_C, e^{Mn}_C, e^{Si}_C, e^{Mn}_{Mn}, and e^{Si}_{Mn} are taken 0.19, −0.012, 0.125, −0.0027, and 0.546[12] at 1873 K, respectively. The value of e^C_{Mn}can be calculated by Eq. 5 [13]:

$$e^C_{Mn} = \frac{A_{rMn}}{A_{rC}} e^{Mn}_C + \frac{1}{230}\left(1 - \frac{A_{rMn}}{A_{rC}}\right) \tag{5}$$

where A_{rC} and A_{rMn} and are the relative atomic mass of C and Mn, respectively.

The value of $e_{Mn}^{C}$is taken -0.0706 in the calculation.

For Fe–C–Mn–Si alloy, the activity coefficient for solute C is [14]:

$$\lg f_{C,L}(T) = e_C^C w(C)_L + e_C^{Mn} w(Mn)_L + e_C^{Si} w(Si)_L \quad (6)$$

The Eq. 7 is used to calculate the $f_i(T)$ under different temperatures[12]:

$$\frac{\ln f_i(T)}{\ln f_i(1873)} = \frac{1873}{T} \quad (7)$$

For Fe–1.21 wt.%C–7.32 wt.%Mn–2.05 wt.%Si alloy, the eutectic reaction temperature T_{met} [14] is:

$$T_{met} = 1421 - 15w(Si) + 3w(Mn) = 1412\,K$$

It can be obtained from Eq. 7 that,

$$\ln f_{i,L}(1412) = \frac{1873}{1412}\ln f_{i,L}(1873) \quad (8)$$

Si enhances the segregation of C and Mn during non-equilibrium solidification [15]. So the segregation of C and Mn in the liquid at the end of solidification increased.

$$\frac{\partial w(C)_L}{\partial w(Si)_L} > 0 \quad (9)$$

$$\frac{\partial w(Mn)_L}{\partial w(Si)_L} > 0, \quad (10)$$

and

$$\frac{\partial w(Fe)_L}{\partial w(Si)_L} = -\left(1 + \frac{\partial w(C)_L}{\partial w(Si)_L} + \frac{\partial w(Mn)_L}{\partial w(Si)_L}\right) < 0 \quad (11)$$

Equation 12 was obtained by differentiating Eq. 3,

$$\begin{aligned}\frac{\partial \Delta G}{\partial w(Si)_L} = &-RT\left\{\left[\frac{-3}{w(Fe)_L} + \frac{1}{w(C)_L} - 0.067\right]\frac{\partial w(C)_L}{\partial w(Si)_L}\right.\\ &+\left[\frac{-3}{w(Fe)_L} + \frac{3}{w(Mn)_L} - 0.061\right]\frac{\partial w(Mn)_L}{\partial w(Si)_L}\\ &\left.+5.385 - \frac{3}{w(Fe)_L}\right\} \quad (12)\end{aligned}$$

i.e.

$$\begin{aligned}&1.21 < w(C)_L < 6.7\\ &7.32 < w(Mn)_L < 20.0\\ &70.0 < w(Fe)_L < 90.0 \quad (13)\end{aligned}$$

From Eqs. 9–12,

$$\frac{\partial \Delta G}{\partial w(Si)_L} \ll 0 \quad (14)$$

Thermodynamic analysis shows that the ΔG for the formation of the $(Fe,Mn)_3C$ in the eutectic decreases with increment Si.

From Table 1, the C content in austenite matrix decreased gradually as the Si content increased. It is seen that the segregation coefficient $(1 - K)$ of Mn increases from 0.140 to 0.163 with the increment of Si. Therefore, the Si enhances the segregation of C and Mn during non-equilibrium solidification.

During solidification, the concentration of C and Mn in the remaining liquid regions between the austenitic dendrites arms and austenitic grains increases continuously because of the segregation of C and Mn. When the liquid in small molten regions attains the concentration of eutectic reaction at the end of the solidification, the nodular eutectics are formed between austenitic dendrite arms and austenitic grains, as shown in Fig. 2.

A new method has been developed to produce an austenitic steel matrix composite with a nodular eutectic reinforcement by using Si to control the solidification structure. The eutectic is formed between austenite dendrite arms and austenitic grains at the end of solidification due to the segregation of C and Mn, which is enhanced by Si. The ΔG for the formation of the $(Fe,Mn)_3C$ in the eutectic decreases with increment of Si, which makes the eutectic reaction more energetically favorable.

Table 1 Effect of Si on the ratio of the dendritic segregation of Mn for the Fe–1.21 wt.%C–7.32 wt.%Mn composite

Quantity of added Si wt.%	C content in austenite matrix	Micro-area	Group 1		Group 2		Group 3	
			Mn	Si	Mn	Si	Mn	Si
0.40 (the fractional percent of Si)	0.93	Cc in center of dendrite, wt.%	7.29	0.48	7.10	0.41	7.25	0.51
		Cb at boundary of dendrite, wt.%	8.35	0.61	8.07	0.47	7.78	0.52
		SR = 1 − K (K = Cc/Cb)	0.13	0.21	0.22	0.13	0.07	0.03
0.80 (the fractional percent of Si)	0.88	Cc in center of dendrite, wt.%	7.10	0.64	7.21	0.68	7.69	0.66
		Cb at boundary of dendrite, wt.%	8.22	0.78	8.73	0.83	8.53	0.81
		SR = 1 − K (K = Cc/Cb)	0.14	0.15	0.17	0.20	0.18	0.19

Note: The compositions were averages of three points

References

1. Venkataraman B, Sundararajan G (1996) Acta Mater 44:451. doi:10.1016/1359-6454(95)00217-0
2. Venkataraman B, Sundararajan G (1996) Acta Mater 44:461. doi:10.1016/1359-6454(95)00218-9
3. Pai BC, Geetha R, Pleeai RM, Satyanarayana KG (1995) J Mater Sci 30:1903. doi:10.1007/BF00353012
4. Yoshiro I, Hidetomo Y, Tomomi H (1995) Wear 181–183:594
5. He Z, Jiang Q, Fu S (1987) Wear 120:305. doi:10.1016/0043-1648(87)90024-X
6. Xu Z, Li T, Li J (2001) J Mater Sci 36:4543. doi:10.1023/A:1017966316060
7. Mao X, Li J, Fu H (1994) Mater Sci Eng A 183:233. doi:10.1016/0921-5093(94)90907-5
8. Xu Z (2002) Mater Sci Eng A 335:109. doi:10.1016/S0921-5093(01)01946-3
9. Li L (1989) Cast alloy and melting. Mechanical Industry Press, Beijing, p 36 (in Chinese)
10. Wei S (1980) Thermodynamics of metallurgical process. Shanghai Science and Technology Press, Shanghai, p 309 (in Chinese)
11. Shi L (1992) Alloy thermodynamics. Mechanical Industry Press, Beijing, p 387 (in Chinese)
12. Dong R (1980) Metallurgical theory. Mechanical Industry Press, Beijing, p 80 (in Chinese)
13. Huang X (1993) Theory of iron and steel metallurgical process. Metallurgical Industry Press, Beijing, p 88 (in Chinese)
14. Zhai Q, Guan S, Shang Q (1999) Theory and application of alloy thermodynamics. Mechanical Industry Press, Beijing, p 50 (in Chinese)
15. Xu Z, Liang G (2006) Metall Mater Trans A 37:3665. doi:10.1007/s11661-006-1060-4